

REINFORCED NOTCHED CROSS-LAMINATED TIMBER PLATES: LOAD-BEARING CAPACITY AND METHODOLOGY FOR PREDICTING THE FORCE IN REINFORCEMENT

Alen Malagic¹, Erik Serrano³, Manfred Augustin¹, Gerhard Schickhofer^{1,2}

ABSTRACT: This paper deals with the estimation of the design force in self-tapping screws used as a reinforcement of notched cross laminated timber plates (CLT). With the reinforcement, apart from an increased load-carrying capacity, a more ductile behaviour of this detail can be achieved. An analytical model based on the Timoshenko Beam Theory was developed, enabling the estimation of the axial force in the reinforcement. A parametric numerical analysis was conducted to verify the model and to provide possible ways for the calibration. The results show a good matching of the model with the numerical results. The load-bearing capacity is analysed using a simple fracture mechanics model taking into consideration the effect of the reinforcement to correctly depict the increase in performance. Theoretical and numerical results are compared with experimental findings and show acceptable correlations encouraging a further development and a subsequent implementation in EN 1995-1-1.

KEYWORDS: reinforcement, self-tapping screw, notches, fracture mechanics, screw stiffness, CLT

1 INTRODUCTION

Unreinforced “notches” in cross laminated timber (CLT) plates (Figure 1), severely reduce the load-bearing capacity of this member and fail in general by delamination in a brittle manner. Hence, they should be generally avoided, and if unavoidable, notches should be reinforced. Since the efforts required for their application are small compared to the increase in the load-bearing capacity, ductility and robustness, an effective way for the reinforcement is the application of fully threaded, self-tapping screws. With this method, beside increased load-bearing capacity even up to the level of the unnotched configuration, also a stabilisation of crack growth and prevention of complete delamination of the plate along the crack plane can be achieved, if the screws are designed accordingly.

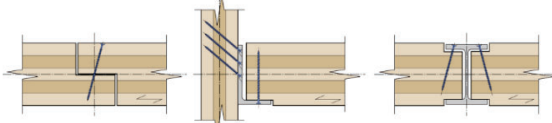


Figure 1: Various types of notches in CLT plates

In addition to mechanical loading the crack initiation and growth can also be caused by climate changes [1]. The geometry of the notch makes the timber in the area of the notch significantly more susceptible to moisture content (MC) variations and hence induced residual stresses. These constant MC variations lead to a crack initiation and with each subsequent MC variation to an increase in

crack length. The crack lengths are relatively small but they tend to increase over time potentially, reaching critical crack lengths and leading to the failure. The reinforcement increases the critical crack length by a factor 2 and improves the overall behaviour [1], thus mitigating the influence of the moisture variations.

At present, as known to the authors, no explicit rules and expressions are given in standards, guidelines, approvals or in the literature for the calculation of the load-bearing capacity of unreinforced as well as reinforced notches in layered timber products like CLT. Nevertheless, it is evident that the layered structure has an influence on the mechanical behaviour of such members. Thus, known approaches developed and valid for unlayered products and beams out of structural timber and glulam are not mechanically consistent as they disregard the influence of the timber fracture properties and the layup. For these reasons a mechanically consistent approach is desired and should be developed.

The development of such approach for the calculation of the load-bearing capacity suitable for the hand calculation is complex. The main difficulty is the constantly changing mode mixity at the crack tip $G_{II} / G_I (\tau_{zx} / \sigma_z)$ as a function of the crack length, therefore complicating the decomposition of the mixed energy release rate (ERR). An attempt to develop such mechanically consistent approach, still applicable for the implementation in standards or guidelines is presented in this paper.

¹ holz.bau forschungs GmbH, Graz, Austria,
alen.malagic@tugraz.at, manfred.augustin@tugraz.at,

² Institute of Timber Engineering and Wood Technology,
Faculty of Civil Engineering, Graz University of Technology,
Graz, Austria, gerhard.schickhofer@tugraz.at

³ Division of Structural Mechanics, Lund University, Lund,
Sweden, erik.serrano@construction.lth.se

2 STATE OF THE ART

2.1 RULES FOR REINFORCED NOTCHED BEAMS IN STANDARDS

Due to the lack of specific rules for CLT, the following review is related to the comparable situation for unlayered timber products (beams) only. Although no related rules are mentioned in EN 1995-1-1:2004/A2:2014 [2], specific sections are given in the German and Austrian National Annex DIN EN 1995-1-1:2010 [3] and ÖNORM B 1995-1-1:2019 [4].

The design force $F_{t,90,d}$, to be carried by the reinforcement, is defined there as a function of the shear force V_d and the notch parameter α . This design approach was developed by Henrici [5] simplifying his findings into the condensed form of Eq. (1).

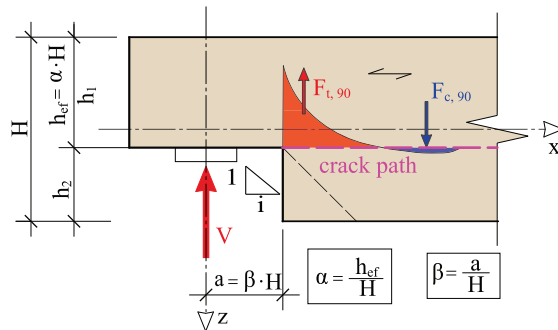


Figure 2: Geometrical parameters of a notched beam [4]

$$F_{t,90,d} = 1.3 \cdot V_d \cdot \left[3 \cdot (1-\alpha)^2 - 2 \cdot (1-\alpha)^3 \right] \quad (1)$$

with V_d ... design value of the shear force, α ...ratio of heights h_{ef}/H

Remark:

To avoid misunderstandings, in the following the denotation for the height ratio α (valid for unlayered timber products) is substituted by ω (valid for layered products like CLT).

In Eq. (1) the force in the reinforcement is calculated by integrating the parabolic shear stresses up to the crack line. The pre-factor 1.3, being a product of the elastic analysis in [5], considers the orthotropy of the timber and the geometry of the notch, leading to conservative values for $\alpha < 0.65$ and $\beta < 0.3$.

Recently, a modified format of Eq. (1) with additional parameters k_α and k_β was proposed in the draft code prEN 1995-1-1:20XX [6] as

$$F_{t,90,d} = k_\alpha \cdot k_\beta \cdot V_d \cdot \left[3 \cdot (1-\alpha)^2 - 2 \cdot (1-\alpha)^3 \right] \quad (2)$$

where

$$k_\alpha = 0.9 + 0.5 \cdot (2\alpha - 1)^2, \quad k_\beta = 1 + 2 \cdot \beta$$

for $\alpha \leq 0.6$ and $\beta \leq 0.2$ the product $k_\alpha \cdot k_\beta$ may be taken as $k_\alpha \cdot k_\beta = 1.3$

As an intermediate summary it can be stated that current methodologies for predicting the force in reinforced notches (of unlayered timber members) disregard several important aspects such as: properties and position of the

reinforcement as well as length of the crack. Thus, a mechanically more accurate and robust approach considering the mentioned parameters is desired and should be developed.

2.2 LOAD-BEARING CAPACITY

Relatively big notches with $\alpha < 0.7$, drastically decrease the load-bearing capacity of notched timber members. By reinforcing them, an increase of the load-bearing capacity by a factor of 1.5 up to 2.5 can be achieved. The failure of the reinforced notch is governed by the axial and the shear capacity of the reinforcement and the splitting strength of the timber respectively. Since the strength of the timber is disregarded in the current design procedures, the load-bearing capacity is proportional to the axial load-bearing capacity of the reinforcement and the number of reinforcing elements. By substituting the axial capacity of the reinforcement in Eq. (1) the failure load at the notch $V_{f,d}$ can be calculated (for unlayered products) as follows:

$$V_{f,d} = \frac{n_{ef} \cdot R_{ax,d}}{1.3 \cdot \left[3 \cdot (1-\alpha)^2 - 2 \cdot (1-\alpha)^3 \right]} \quad (3)$$

with $n_{ef} = n$ and $R_{ax,d}$... design value of the axial load-carrying capacity per screw

The strength of the timber is indirectly considered in a proposal authored by Dietsch [7] and also mentioned in prEN 1995-1-1:20XX [6]. The load-bearing capacity there is limited to twice the value of the unreinforced notch. This simple and practical proposal for standards is based on insights made in [1] on a basis of extensive experimental test results and the theoretical insights regarding the fracture energy in pure mode II failure. However, an implementation in this form is questionable for highly orthotropic products such as CLT due to the increased influence of the rolling shear behaviour. Significant discrepancies between the load-bearing capacity calculated by Eq. (3) and experimental results were observed in [1] and [10]. The Eq. (3) provided unsafe results in some configurations. Placing a large amount of reinforcements at the notch can cause this disagreement due to the shift of the failure mode from the reinforcement to the failure at the notch by excessive cracking and subsequent delamination. In CLT notches this fact transforms to: failure in the screw (underreinforced), failure due to the splitting of the timber at the crack tip (overreinforced) and failure due to the splitting and simultaneous failure of the screw (balanced). Naturally, the balanced case is hardly achievable.

The predictions by Eq. (3) have been also compared with the experimental results conducted on reinforced notched CLT plates, see chapter 5.

The load-bearing capacity of reinforced notches in beams was investigated by Jockwer ([1], [8]), proposing an analytical model based on energy balance method of *Linear Elastic Fracture Mechanics* (LEFM). The total energy release rate (ERR) in the mixed fracture mode was evaluated and then a mode partitioning according to the approach from Riipola [9] was applied. A pronounced influence of the crack shearing (mode II) with increasing

crack length and α -value was noted, leading to the reported increase of the load-bearing capacity. The increase of the load-bearing capacity by a factor of about 2 reported in [1] corresponds well with around 4 times larger fracture energy in pure mode II leading to increase in the load-bearing capacity $\sqrt{G_{II}/G_I} \approx 2$ according to LEFM.

A more detailed approach is given by Sorin et. al. [10]. The load-bearing capacity of the notch is calculated according to the *Equivalent Linear Elastic Fracture Mechanics* (Equiv. LEFM) taking into account the quasi-brittleness of the timber and employing crack growth curves (R curves). The linear elastic calculations are made iteratively on different crack lengths. Each crack length has a unique crack growth resistance in separate fracture modes. This model can accurately predict the force evolution and failure load as a function of the crack length, however on the cost of simplicity when compared to [8].

The increase of the load-bearing capacity of reinforced notches can be vividly illustrated by an analogy regarding the timber anatomy: It is a well-known occurrence during the testing of fracture properties on timber specimens that the presence of knots along the fracture plane cause an increase in fracture energy and failure load of the tested specimen. Such specimens are not desired in the analysis and will be commonly disregarded but show a positive influence of knots on the fracture parameters. The knots in such cases are carrying forces between the cross sections divided by the crack and therefore lead to an increase in system stiffness and fracture energy. A similar effect can be achieved by placing self-tapped screws at the notch.

2.3 FORCE IN THE REINFORCEMENT

Literature references regarding the calculation of the design forces in the reinforcement at the notch – in particular for layered timber products – are rather scarce, if not missing. An analytical model for unlayered notched beams based on the Timoshenko Beam Theory was presented in Jockwer [1]. As known to the authors, no other paper of such matter is present, consequently there is a need for further investigations on this topic.

3 METHODOLOGY FOR PREDICTING THE FORCE IN REINFORCEMENT

In the chapters 3 and 4 diagrams regarding the force in reinforcement and the load-bearing capacity of notched CLT plates will be shown. All presented diagrams are related to a reference case in order to clearly present results and parameter relations. The reference case is a 5-layered CLT-plate with the layout: 30-30-30-30-30 mm (underlined numbers indicate the thickness of cross-layers). For a consistent comparison a constant parameter $\beta = 0.5$ was chosen. In all presented diagrams dashed lines refer to the analytical beam model (section 3.1 and 4.1), while solid lines refer to the numerical model (section 3.2).

3.1 ANALYTICAL MODEL

The analytical model is based on the Timoshenko Beam Theory. The used system is graphically depicted in Figure 3. For the application of the model a crack-length L_{crack} has to be pre-assumed. The screw (group) is substituted by spring element of equivalent stiffness. However, to enable a closed form solution, the lateral screw stiffness is ignored. The impact of this simplification is further investigated in the scope of the numerical parametric analysis.

The axial stiffness for part of the single screw under/above the crack is calculated according to Eq. (4) from Ringhofer [11]. The axial stiffness of the whole screw K_{ser} is calculated taking into account the series effect acting on the screw because of the crack.

$$K_{ser,i} = k_{ax} \cdot 160 \cdot \left(\frac{\rho_{12}}{420} \right)^{0.85} \cdot d^{0.9} \cdot l_{ef,i}^{0.6} \quad (4)$$

with $k_{ax} = 1.0$ for $\alpha = 90^\circ$, ρ_{12} ... density at moisture content $u = 12\%$ [kg/m^3], d ... diameter of the screw [mm], $l_{ef,i}$... penetration length of the screw in timber under the crack and above the crack [mm], $K_{ser,i}$... axial stiffness for part of the screw under/above the crack interface resp. [N/mm]

Remark: The stiffness of the screw group is given as: $K_{ser} \cdot n_{screw}$, where n_{screw} ... number of screws, K_{ser} ... stiffness of the whole screw

The forces in the reinforcement are calculated by applying the principle of virtual forces on the first order statically indeterminate system shown in Figure 3.

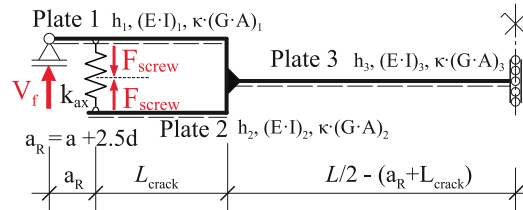


Figure 3: Analytical beam model

After simplification the axial force in the reinforcement $F_{t,90,d}$ in the notched CLT plate of width w is as follows:

$$F_{t,90,d} = \frac{\frac{L_{crack}^2}{6 \cdot EI_1} \cdot (3 \cdot a_R + 2 \cdot L_{crack}) + \frac{L_{crack}}{GA_1}}{\frac{L_{crack}^3}{3} \cdot \left(\frac{1}{EI_1} + \frac{1}{EI_2} \right) + \frac{1}{k_{ax}} + \left(\frac{1}{GA_1} + \frac{1}{GA_2} \right) \cdot L_{crack}} \quad (5)$$

3.2 (PARAMETRIC) NUMERICAL MODEL

In order to verify the analytical model from section 3.1 a parametric numerical analysis was conducted. In its frame 3-, 5- and 7-layered CLT plates were investigated. The calculation was elaborated using the finite element software package ANSYS APDL 2021 R1. For ease of work, sets with a range of parameters were submitted as batch file to the solver. Detailed information regarding the considered layouts are given in Table 1. The geometry, loading and boundary conditions of the analysed model are illustrated in Figure 4.

A plane stress model was applied on the plate width $w = 600$ mm to match the width of CLT plates from experimental tests. The plate is loaded by a point load in the symmetric mid span 3-point bending configuration. The support is modelled by means of a steel plate to avoid singularity and unrealistic deformations. It is restrained in the Z-direction and free in X-direction, with free rotation about the Y-axis (Figure 4). A global mesh size of 5 mm was used, while the local mesh refinement at the crack tip and along the crack interface was applied in sizes of 1.5 to 2.0 mm. The material model is linear elastic orthotropic represented by the properties given in Table 2.

Table 1: Parameters used in the numerical analysis

| Input and analysis parameters for the analytical and numerical models | | | |
|---|---|--|---|
| Num. of layers | 3 | 5 | 7 |
| Layup ^{a)} [mm] | 40- <u>40</u> -40 | 30- <u>30</u> -30- <u>30</u> -30 40- <u>20</u> -40- <u>20</u> -40 40- <u>20</u> -20- <u>20</u> -40 40- <u>40</u> -40- <u>40</u> -40 | 30- <u>30</u> -30- <u>30</u> -30 30- <u>30</u> -30 30-30-30- <u>30</u> -30-30 |
| ω [-] | $0.5 \leq \omega < 1.0$ | | |
| β [-] | 0.25, 0.5, 1.0 | | |
| L_{crack} [mm] | $2.5 \cdot d_{screw} \leq L_{crack} \leq 2 \cdot H_{plate}$ | | |

^{a)} Underlined numbers indicate the thickness of cross layers

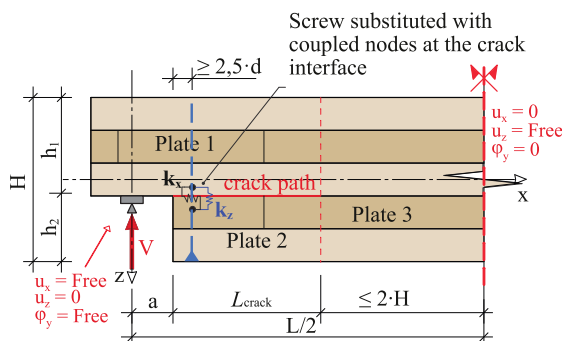


Figure 4: Illustration of the (parametric) numerical model

Due to the application of a plane stress model the screw could not be considered as a beam element. Instead, a coupling of the nodes with spring elements at the crack interface was applied. The number of parameters to be considered for the definition of the numerical model in a notched layered member is significantly higher compared to the notched beams made of structural timber or glulam. For example, the parameters defining the number of layers and the layup of the CLT plate need to be defined in addition. Subsequently, the complexity of the parametric analysis, as well as the needed computational time increase exponentially.

Table 2: Material properties used in the numerical analysis

| Parameter | Value | Description |
|-------------|--------|---|
| E_0 | 11000; | MOE longitudinal; transversal [MPa] |
| E_{90} | 390 | |
| $G_{0,90}$ | 690; | Shear modulus, longitudinal; transversal [MPa] |
| $G_{90,90}$ | 69.0 | |
| $G_{c,I}$ | 0.30; | Critical energy release rate, Mode I; Mode II [mJ/mm ²] |
| $G_{c,II}$ | 0.90 | |
| ν_{LR} | 0.56; | Poisson ratios [-] |
| ν_{RT} | 0.03 | |

In the present analysis the number of considered parameters was reduced by introducing several assumptions in line with the features of CLT-plates and construction practice: The most relevant adoption was made involving the type of reinforcement used in notched CLT-plates as well as the configuration of the reinforcement. Due to the relatively small thickness of the CLT-plate and a width of up to 3 m, the only feasible way of reinforcing such elements in practice is the application of self-tapping screws. In line with the proposals in [7] the reinforcement should be placed in one row and at a distance of about $2.5 \cdot d_{screw}$ from the notch face to the screw. Moreover, the width of the CLT-plates requires a maximum screw distance in a row to be defined. Otherwise, a crack propagation between the screws may occur, severely reducing the load-bearing capacity. In this work a maximum screw distance of 150 mm is proposed and considered. This distance is in line with the situation in practice, however, a maximal distance should be determined on the basis of experimental tests. Screws of the nominal diameter $d = 8$ mm and a length equal to the plate thickness with an inclination angle of $\alpha = 90^\circ$ were assumed for the reinforcement in this work. With the mentioned assumptions the stiffness of a group of screws can be defined. The axial screw stiffness was considered as given by Eq. (4).

In the numerical model the fracture parameters at the crack tip were obtained as a function of the crack length. The total (mixed) energy release rates and respective modal contributions in the modes I and II were evaluated with the built-in software module “Virtual-crack-closing-technique” (VCCT). To verify the mixed ERR from VCCT the J-integral was applied in the numerical analysis. The modal contributions were verified with the ratio of shear and normal stresses (τ_{zx} / σ_z) giving the mode mixity ratio G_{II} / G_I . The verification calculations for the total ERR showed no difference to the VCCT method and mode partitioning showed minor differences but the same tendency in results.

3.3 FORCES IN THE REINFORCEMENT

Predictions for the forces in the reinforcement were computed at specific positions for different notch heights as illustrated in Figure 5.

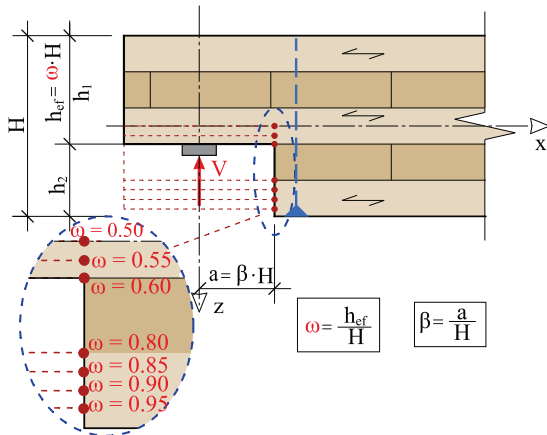


Figure 5: Positions of notches used in comparison

The notches in the CLT have a special failure mode when the notch is situated in a transversal layer: The crack there propagates under an angle of approximately 45° up to the layer interface and then continues along the interface [12]. As a consequence, the transversal layer should be excluded from the calculations of the load-bearing capacity in the notched CLT-plates and also excluded from the predictions of the force in the screw, Eq. (5).

The reinforcement leads to an exchange of forces between the upper and lower part of the plate. This exchange depends on the geometry parameters of the notch (ω , β), but also on the crack length L_{crack} and the stiffness of the screw.

In Figure 6 the results from the numerical and analytical analysis regarding the influence of the crack length on the force in the screw are depicted.

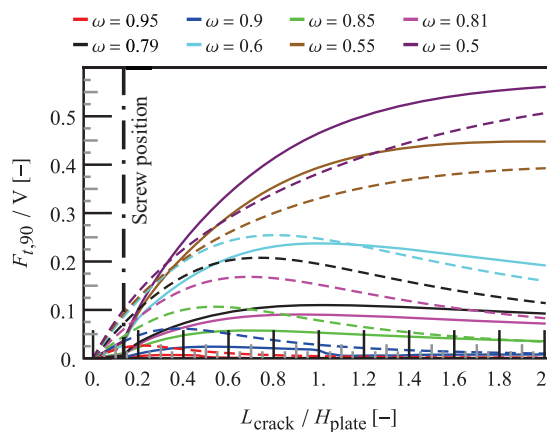


Figure 6: Axial force in the screw depending on the crack length (dashed lines ... analytical model, solid lines ... numerical model)

The analytical and the numerical model show a comparable tendency of an increasing force in the reinforcement with an increasing crack length. This was verified for all investigated ω -values. Additionally, it can be recognised that for bigger crack lengths a decreasing

trend in the force of the screw may occur. This can be explained by the fact that the stiffness of the system decreases with an increasing L_{crack} . In the analytical model the point of the local maximum could be obtained by applying the condition $dF / dL_{\text{crack}} = 0$. However, this point is not of practical relevance for the design of the reinforcement.

The crack propagation is initiated at the notch tip “behind” the position of the screw. However, until the crack passed the screw position no force, or even compression forces, in the screw were observed. Thus, forces at $L_{\text{crack}} = 0$ are assumed to be zero in the numerical analysis.

Jockwer [1] mentions the possibility of an interaction between the member parts under and above the crack in reinforced notches during the crack growth. This occurrence renders the analytical model inappropriate due to the assumption, that the crack interface is not in contact. This assumption was investigated in the numerical model by defining contact elements along the opening crack interface. Within the inspected layouts from Table 1 a consistent behaviour could be recognised. The interaction at the crack interface occurs for larger crack lengths and small notches of up to $h_2 = 15$ mm. The analytical model in this range of ω shows conservative results in comparison to the numerical one. This is noted on all inspected CLT layouts, therefore the applicability of the taken assumption in the analytical model is acceptable.

As mentioned, the failure of reinforced notches can occur due to the pull-out of the reinforcement. In order to determine the occurring failure mode in the analysed notches the predicted force in the reinforcement for the screw group was compared with their load-bearing capacity determined as

$$\left(\frac{F_{ax,Ed}}{F_{ax,Rd}}\right)^2 + \left(\frac{F_{v,Ed}}{F_{v,Rd}}\right)^2 = 1. \quad (6)$$

with $F_{ax,Rd}$, $F_{v,Rd}$... axial and lateral load-bearing capacity of the screw group

The load-bearing capacity was determined according to the expressions given in EN 1995-1-1 [2], sections 8.3 and 8.5. The detailed calculation is excluded here for simplicity. The acting shear force is taken from the numerical analysis and was included in Eq. (6). In order to simplify the results, the maximal shear force obtained for each ω was used.

The resulting load-bearing capacity for the screw group is illustrated in Figure 7. Their failure load capacities are significantly higher than the maximal forces in the reinforcement for the relevant crack lengths, i.e. pointing out a low risk of screw pull-out during the crack propagation. This leads to the “over-reinforced” case of the notch; hence the failure in the timber occurs due to crack propagation. This hypothesis is questioned on the basis of the experimental results in chapter 5.

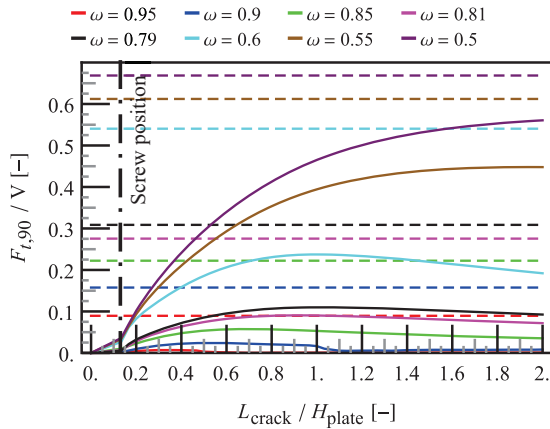


Figure 7: Comparison of the axial force in the screw to the load-bearing capacity of the applied screws group depending on the crack length (solid lines ... numerical model, dashed lines ... load-bearing capacity of the screw group, Eq. (6.))

In contrast to the axial force $F_{t,90}$, the shear force F_v shows a constant increase of the force in the screw with increasing crack length (Figure 8). Thus, the load-bearing capacity of the reinforcement in shear is relevant for the determination of the load-bearing capacity of the notched CLT plate for larger notch parameter β and larger crack lengths. The main goal of a reinforcement is to reduce and limit the crack opening at small crack lengths. However, that increases the shear loading at the crack and induces a mode II failure at the crack tip. In order to further increase the load-bearing capacity, the shear loading at the crack should be reduced by increasing the lateral stiffness of the screw. This is accomplished, e.g. by inclining the screws at an angle to grain below 60° ([1],[8]).

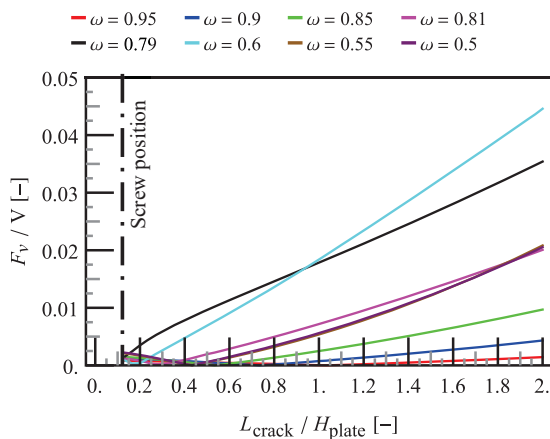


Figure 8: Shear force in the screws depending on the crack length (numerical model)

An interesting occurrence can be recognised in the distribution of the shear force: The maximum shear force in the reference case is obtained for $\omega = 0.6$ and $\omega = 0.79$ instead of $\omega = 0.5$ as expected from the distribution of the axial forces. This occurs at the interface of the transversal and longitudinal layer due to the increased compliance caused by rolling shear in the transversal layer. This

implies a bigger influence of the mode II failure at the interface of the layers, cf. section 4.2.

The influence of the parameter β on the axial force in the screw is illustrated in Figure 9. The crack length in the analysis was assumed as $L_{crack} = 150$ mm. This assumption is based on observations from experimental tests conducted by the author ([12]) and found in literature [1] respectively, as the approximate, where a failure of the reinforced notch occurred. The chosen length refers to failures in cases, where inclined screws were used. The lengths for non-inclined screws are smaller and can be expected in the region of 80 to 100 mm. However, a bigger crack length was chosen for the analysis in order to obtain more conservative results.

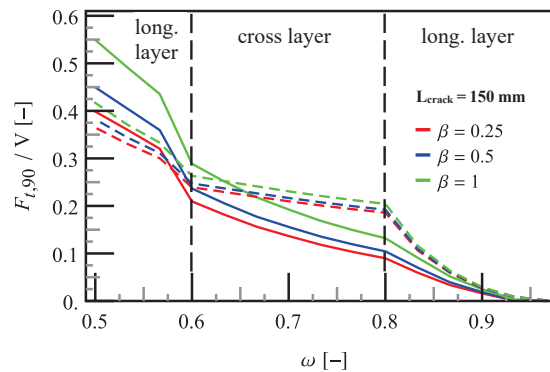


Figure 9: Axial force in the screw for $L_{crack} = 150$ mm depending on the parameter ω and β (dashed line ... analytical model, solid line ... numerical model)

It can be seen that the analytical model is conservative in the area of the first longitudinal and transversal layer ($\omega \geq 0.6$), but with an increasing notch height the results diverge to the unsafe region compared to the numerical results. This was observed for all considered layups. The differences in the reference case are equal to 15% of the force at the support; for other lay-ups the differences grow up to 25%. As a consequence this implies that the analytical approach should be applied only in the region $\beta \leq 0.5$. Alternatively, a correction factor increasing the effective notch length as a function of β could be applied.

3.4 COMPARISON OF DIFFERENT METHODS AND VERIFICATION

In this section a comparison of methods for the prediction of the force in the reinforcement related to the reference configuration is given. Beside the analytical and numerical method explained in the sections 3.1 and 3.2, also present methods for unlayered notched beams (see section 2.1; Eq. (1) and (2)) were included, although they are not mechanically consistent with the layered timber product CLT.

A comparison of the results for the axial force in the screw between the analytical and numerical approach is shown in Figure 10. With an increasing crack length, the analytical model converges to the numerical one. This behaviour can be explained due to the assumptions made

in the Timoshenko Beam Theory characterised by a dominant shear deformation of the cracked plate parts under and above the crack interface for small crack lengths and small notch heights. Improved results can be obtained by increasing the effective crack length to overcome the restrictions of the beam theory. In general, the predictions of the analytical model significantly overestimate the forces in the reinforcement predicted by numerical model. On the other side for $\omega < 0.6$ the analytical model underestimates forces in numerical model in range of 20%. These differences are significant and can't be neglected, therefore further investigation and refinement of the model is needed!

In Figure 10 for $\omega = 0.95$ and 0.9 the roughness of the curves is noted. The roughness is caused by the predictions in the numerical model. In mentioned range, the crack interface is in contact and it is causing constant change in force in the screw in contrary to assumption of analytical model.

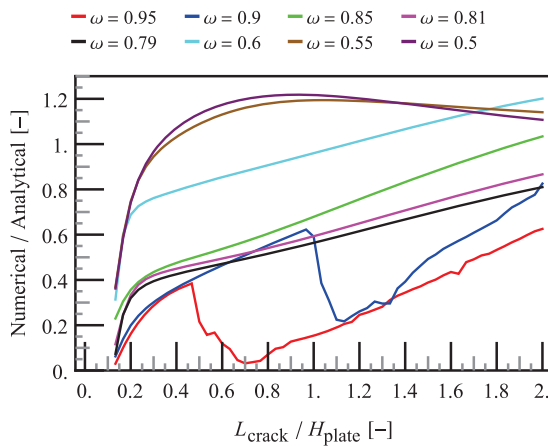


Figure 10: Comparison of the axial force in the screw between the numerical and analytical model for the reference configuration

A comparison of different methods for the prediction of the force in the screw of the reference CLT plate is shown in Figure 11. The analytical and numerical solutions were computed for the crack lengths $L_{crack} = 100$ mm and 150 mm, i.e. in the domain relevant for failure of the notch (cf. section 3.3). In order to check their applicability, although the methods are not consistent with the layered timber products like CLT, in addition results for the regulations valid for unlayered notched timber products specified in the National Annexes [3] and [4] to EN 1995-1-1 and the current draft prEN 1995-1-1:20XX [6] are included.

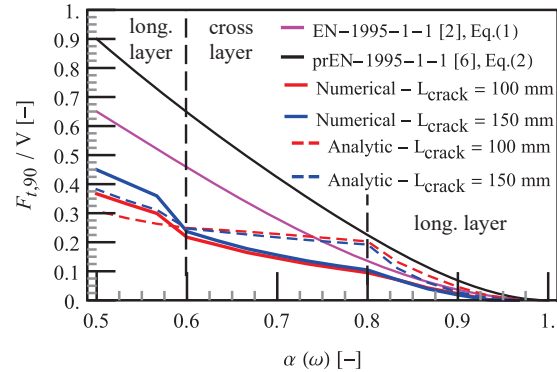


Figure 11: Force in the screw according to different methods for different parameter ω and $\beta = 0.5$

In the draft prEN1995-1-1:20XX [6] (Eq. 2) a new approach for the calculation of the force in the reinforcement is specified as described in section 2.1. This method is compared with the regulations in the National Annexes in [3] and [4] (Eq. 1) (Figure 12). It can be recognised that the new approach in the draft standard leads to substantially higher forces in the reinforcement for the full range of the investigated parameter α and β .

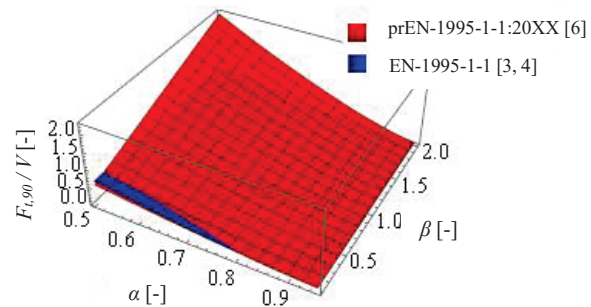


Figure 12: Illustration of the force in the reinforcement (screw) depending on the parameter α and β for the methods in [3], [4] and [6] resp.

In Table 3 a comparison of results for different layups applying the mentioned methods is listed. The analytical model and the numerical model for CLT show a good match. The approaches in [3], [4] and [6] resp. are leading to very conservative results, which was expected as these methods are not considering the layered structure of CLT and the influences of cracks, as well as the reinforcements are not taken into account.

If the stiffness of the screw is ignored, the results of the analytical method for the prediction of the force in the reinforcement of CLT plates, Eq. (5), is approaching the results in the National Annexes to the standard EN-1995-1-1, [3] and [4]. This can be achieved by assuming an infinite stiffness for the screw. Further the crack length is assumed again as $L_{crack} = 150$ mm. The results over the complete range of the important parameters ω and β are presented in Figure 13. If an infinite stiffness of the screw is assumed, the results of the analytical model lead to increased forces in the screw in an expected range of 20% to 30% for all analysed configurations.

Table 3: Comparison of results for the prediction of the force in the screw according to the different methods and different layups; parameter $\beta = 0.5$ and crack length $L_{crack} = 150$ mm (results are normalised to $F_{i, 90} / V$; the comparison is given in % and normalised to the numerical solution)

| Method | Layup | | | |
|------------------------|-------------------------|-------------------------|-------------------------|---------------------------|
| | 40-20-20-20-40 mm | | 30-30-30-30-30-30 mm | |
| | $\alpha(\omega) = 0.57$ | $\alpha(\omega) = 0.50$ | $\alpha(\omega) = 0.57$ | $\alpha(\omega) = 0.43^*$ |
| | $F_{i, 90} / V [-]$ | | $F_{i, 90} / V [-]$ | |
| Analytical model - CLT | 0.29 (+26%) | 0.37 (-16%) | 0.36 (-5%) | 0.38 (-15%) |
| Numerical model - CLT | 0.23 | 0.44 | 0.38 | 0.45 |
| prEN 1995-1-1:20XX | 0.72 (+213%) | 0.90 (+104%) | 0.72 (+90%) | 1.09 (+142%) |
| EN 1995-1-1 | 0.51 (+121%) | 0.65 (+47%) | 0.51 (+34%) | 0.78 (+73%) |

* $\alpha(\omega) = 0.43$ is used as $\alpha(\omega) = 0.5$ is situated in a transversal layer

With the increased forces considering an infinite stiffness of the screw the results match better with the approach in the National Annexes (Eq. 1). However, these results underestimate the level of the force in the first layer of the CLT and overestimate the force at the top of the transversal layer. The matching of the methods depends heavily on the layups, but in general the differences are small for $\beta < 1.0$. It can be concluded that the mentioned procedure can be used for standardisation, but in addition the influence of the CLT layup should be taken into account by a fitting factor.

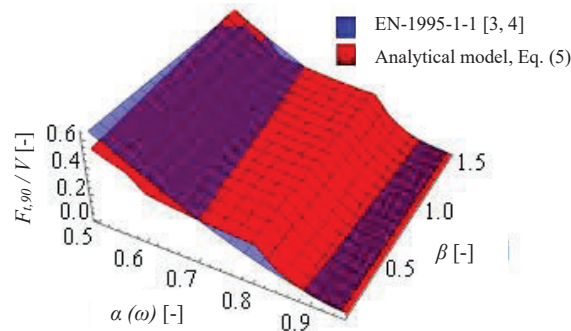


Figure 13: Comparison of the force in the screw according to [3], [4] and the analytical model (assuming a crack length $L_{crack} = 150$ mm) for different parameter β , α and ω respectively

4 LOAD-BEARING CAPACITY

In comparison to the unreinforced notches in CLT the development of mechanically consistent model but also appropriate for hand calculation for reinforced case is more difficult. Due to the pronounced mixed mode failure in reinforced notches a failure criterion needs to be considered.

In this chapter the basics for the computation of the load-bearing capacity of the reinforced notched CLT-plate will be briefly described. The proposed model is based on the

energy balance method of LEFM considering all important parameters influencing the load-bearing capacity. Furthermore, assumptions of the critical crack length need to be made for hand calculations with the analytical model.

4.1 ANALYTICAL MODEL FOR THE PREDICTION OF THE MODE MIXITY AND LOAD-BEARING CAPACITY IN REINFORCED CLT-PLATES

The total energy release rate (ERR) of the system in Figure 3 in the frame of the LEFM (expecting a brittle failure in the interface) is given as:

$$G_m = \left[\left(\frac{M_1^2}{EI_1} \right) + \left(\frac{M_2^2}{EI_2} \right) - \left(\frac{M_3^2}{EI_3} \right) \right] + \left[\left(\frac{V_1^2}{\kappa GA_1} \right) + \left(\frac{V_2^2}{\kappa GA_2} \right) - \left(\frac{V_3^2}{\kappa GA_3} \right) \right] \quad (7)$$

where

- κGA_i , shear stiffnesses for the plate parts 1, 2, 3
- EI_i , bending stiffnesses for the plate parts 1, 2, 3
- M_i, V_i moment and shear forces at the crack tip of the plate parts 1, 2, 3

The main challenge regarding Eq. (7) is to decompose it in modal ERR constituents, i.e. mode I and mode II respectively. In the literature the mode decomposition of unlayered cross sections as well as for laminates is well researched. In the pioneering work of Williams [15] a so called “global method” of decomposition was developed. Williams proposed a partitioning method based on the assumptions that: (i) a pure mode I exist when opposite moments act on the plates above and below the crack; and (ii) a pure mode II is obtained when the curvature in the two plates separated by the crack is the same. Such assumptions, however, lead to incorrect results when they are applied to laminates with unsymmetric layups and layers not of the same thickness. For that reason, the accuracy of Williams theory is often questioned when applying it to laminate cross sections such as CLT. The applicability of Williams method was briefly investigated in the scope of this paper. A mode decomposition showed a good matching for the symmetric case with $\omega = 0.5$, but greater deviations for $\omega \neq 0.5$ compared to the numerical model were observed.

The mode mixity is evaluated as a function of the crack length with the numerical method based on VCCT. The numerical approach is considered as a reliable method for the analysis of fracture properties and mode mixity. Nonetheless, an analytical approach was also developed for easier handling of the parameters and to verify the possibility of using an analytical model for the mode decomposition.

“An Elastic Interface Model for Coupled Laminates” developed by Bennati [16] was used to derive the mode mixity in notched CLT plates. The model is based on the Timoshenko Laminate Theory. The solution is derived based on the crack tip element (CTE) illustrated in Figure 14. The CTE includes the crack tip and a part of the beam behind the crack tip. The CLT laminate is divided by a crack interface into two sublaminates, which are coupled with continuously distributed linear elastic springs

enabling a better description of the deformation at the crack tip. This step requires a fitting with experimental or numerical results. The sensitivity of the spring stiffness on mode mixity was analysed and it has been shown that for $k_z > 1000$ N/mm the mode mixity is constant, therefore $k_z = 1000$ N/mm was taken. To include the influence of transversal layers, the stiffness k_x was defined as $k_z / k_x = 10$. The strain, displacement and stress distributions in the CTE are derived by simultaneously solving a set of two differential equations which define the interface stresses. Then, the mixed energy release rate and its mode I and mode II contributions are evaluated based on Rice's J-integral. The solution of this integral for the total ERR in mode I and II is given in Eq. (8)

$$G_I = \frac{\sigma_z^2}{2 \cdot k_z} \quad G_{II} = \frac{\tau_{zx}^2}{2 \cdot k_x} \quad (8)$$

with
 G_I, G_{II} ERR in mode I and II [mJ / m²]
 k_x, k_z spring stiffness in the horizontal (x) and the vertical (z) direction
 σ_z maximum normal stress at $x = 0$ (crack tip) in direction perpendicular to grain
 τ_{zx} maximum shear stress at $x = 0$ (crack tip)

The mode mixity is represented as the phase angle $\psi = \arctan(\sqrt{G_{II}} / G_I)$ where $\psi = 90^\circ$ refers to the pure mode II and $\psi = 0^\circ$ to the pure mode I fracture.

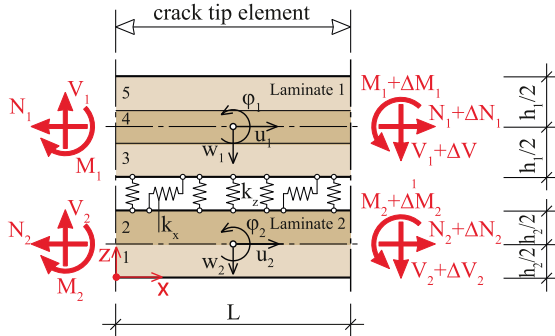


Figure 14: Crack tip element (CTE) - Elastic Interface model

4.2 FRACTURE BEHAVIOUR OF REINFORCED CLT NOTCHES

The distribution of the mode I ERR (G_I) as a function of the crack length normalized to the height of the plate is shown for the reference case in Figure 15. The diagram clearly shows the decreasing tendency of the G_I with an increasing crack length. For comparison the G_I in unreinforced notches is causing the failure of the notch as G_I increases with a crack length leading to the failure at relatively small crack lengths of around 50 mm.

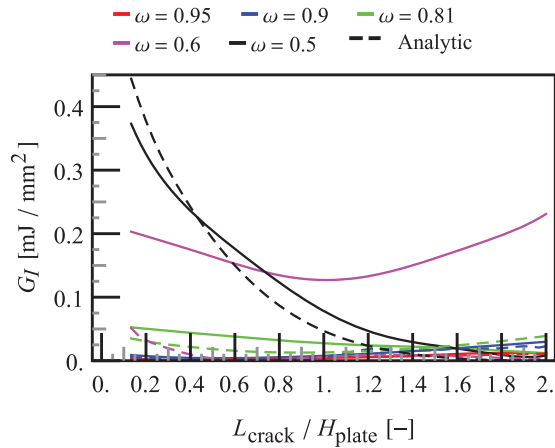


Figure 15: ERR in mode I for the reference layout

The effect of the reinforcement is clearly recognisable as the reinforcement reduces the cracking tendency of the plate, as it reduces the crack opening and hence the mode I influence. This effect is increasing with stiffer reinforcements. The agreement of the analytical and numerical model for G_I is relatively poor, especially at the interface between the longitudinal and transversal layer mainly due to the influence of significantly different shear and elastic modulus between them. However, G_I shows the same tendency for all notch heights in the numerical model, excluding the solution at the interface.

The distribution of the mode II ERR (G_{II}) is shown in Figure 16. In this case the G_{II} increases with the crack length. Again, for the same reason the agreement with the numerical model is poor at the interface. Otherwise, a good agreement between the models was observed.

The increasing mode II is also present in the unreinforced notches [1], but the ratio G_{II} / G_I is significantly lower compared to the reinforced case. Moreover, the value of G_{II} doesn't influence the load-bearing capacity of the unreinforced notches significantly as the fracture energy in mode I is up to three times lower compared to that of mode II.

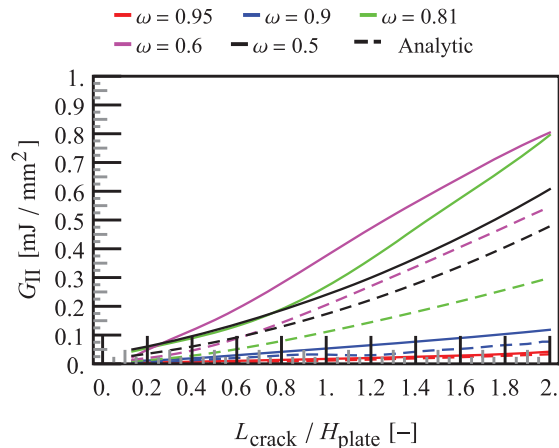


Figure 16: ERR in mode II for the reference layout

The load-bearing capacity of reinforced CLT notches is heavily dependent upon the dominant mode of fracture. Therefore, the plots of the mixed mode ratio and mode mixity were investigated. The mixed mode ratio for mode I is shown in Figure 17. It can be seen that the share of the mode I in total mixed mode ERR (G_{mixed}) shows a descending tendency when a reinforcement is applied. This decreasing tendency is especially pronounced in the range $\omega = 0.5$ to 0.6 , where for smaller crack lengths the mode I failure is dominant. The decrease of G_I is mainly responsible for the significant increase of the load-bearing capacity in reinforced notches (see Table 4).

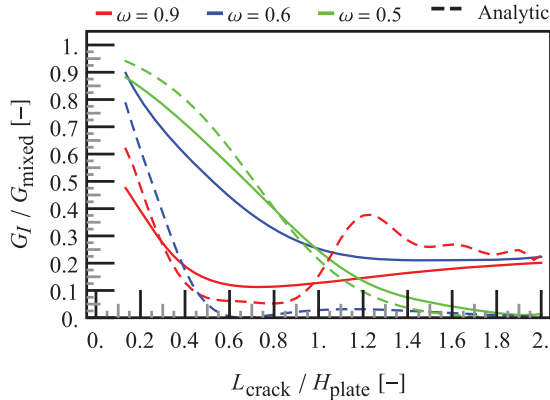


Figure 17: Mixed mode ratio of mode I for reference layout

For big ω -values the mode II is dominant, already at small crack lengths. For larger crack lengths they converge to constant value (Figure 18). It is noted that for $\omega = 0.9$ and large crack lengths the delaminated parts of the plate are in contact, therefore producing a significant portion of mode II.

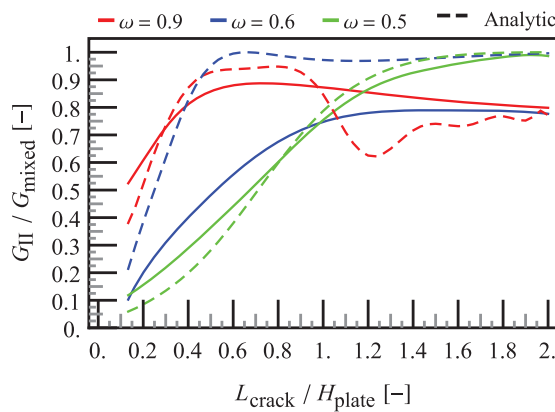


Figure 18: Mixed mode ratio of mode II for reference layout

Two plots of the mode mixity are shown with the intention to investigate the influence of the force in the screw on the mode mixity and subsequently on the load-bearing capacity. The Figure 19 and Figure 20 refer to the solution with forces from the numerical and analytical analysis respectively.

It can be seen that the force in the screw plays a big role on the accuracy of the mode mixity. To increase accuracy, a correction factor for Eq. (5) can be developed.

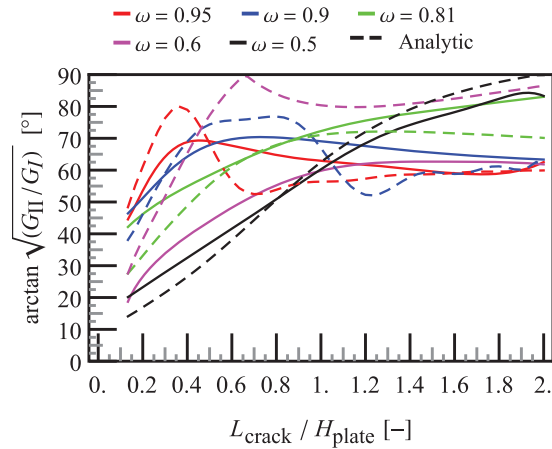


Figure 19: Mode mixity of the reference layout with forces in the reinforcement from the numerical analysis

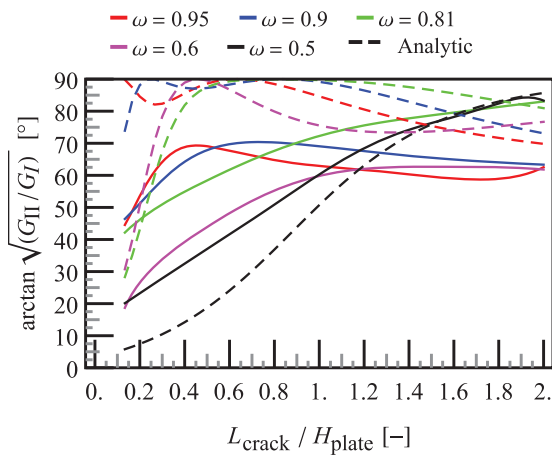


Figure 20: Mode mixity of the reference layout with forces in the reinforcement from the analytical solution

4.3 LOAD-BEARING CAPACITY

The load-bearing capacity of a reinforced CLT notch can be explicitly calculated applying Eq. (7) if the mode mixity is known. For that reason, an effort is made in the following to determine the mode mixity. The closed form solution of the mode mixity can't be defined with an expression which would be suitable for the application in standards. Therefore, a regression curve can be developed based on important geometric parameters (ω , β) and the CLT layout. The significant mode mixity of the reinforced beam in failure endorses the implementation of a failure criterion. In Eq. (9) a semi-quadratic criterion was used. However, other failure criteria could also be appropriate.

$$\left(\frac{G_I}{G_{I,c}}\right) + \left(\frac{G_{II}}{G_{II,c}}\right)^2 = 1 \quad (9)$$

with $G_{I,c}$ and $G_{II,c}$ critical ERR in mode I and II, respectively

The solution of Eq. (9) is illustrated in Figure 21.

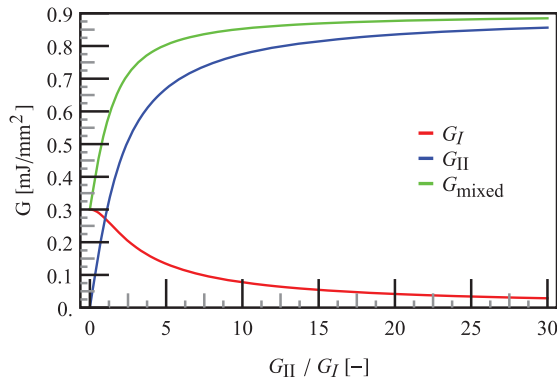


Figure 21: Progression of the critical ERR in mode I, II and mixed mode G_{mixed} as a function of G_{II} / G_I

Next, a brief methodology for the determination of the load-bearing capacity for the proposed analytical model is given.

- (i) Determine the force in the screw applying Eq. (5), assuming $L_{crack} = 150$ mm – a conservative approximation compared to $L_{crack} = 100$ mm.
- (ii) Obtain the phase angle of the mode mixity from a regression curve obtained from the analytical or numerical model. In the regression curve a critical crack length should be assumed – proposal from experimental results in this work and from literature for not inclined screws is $L_{crack} = 100$ mm
- (iii) Determine from Eq. (9) or with a regression curve the critical mixed mode ERR G_{mixed} and calculate the load-bearing capacity with Eq. (10)

$$V_{f,d} = \sqrt{\frac{2 \cdot w \cdot G_{mixed}}{\left(\frac{(1-\eta)^2}{(\kappa GA)_1} + \frac{\eta^2}{(\kappa GA)_2} - \frac{1}{(\kappa GA)_3} \right) + H \cdot \left(\frac{(1+\beta-\eta)^2}{(EI)_1} + \frac{\eta^2}{(EI)_2} - \frac{(1+\beta)^2}{(EI)_3} \right)}} \quad (10)$$

where
 $\eta = F_{t,90} / V_d$

5 EXPERIMENTAL RESULTS AND VERIFICATION

For the analytical method described in the previous section a comparison of the predicted load-bearing capacity with experimental results presented in [12] was prepared. The summary of the conducted experimental tests on reinforced notched CLT plates is illustrated in Table 4. For determining the mode mixity the results from Figure 19 were taken, as a better matching was obtained. The comparison showed conservative predictions of the model in a range of 10% to 17% (Figure 22). The results show that this method can be used to explicitly predict the failure load of reinforced notched CLT plates. It should be noted that the analytical method for the prediction of the force in the screw and also Elastic Interface model can be utilised for solid timber or glulam beams.

Table 4: Detailed overview of experimental tests on reinforced notched CLT elements

| Layup [mm] | Series | n_{screws} | Screw angle α / β [°] | $V_{f,mean,unreinforced}$ [kN] | $V_{f,mean,reinforced}$ [kN] | $V_{f,reinf}/V_{f,unreinf}$ | |
|-------------------------|--------|--------------|----------------------------------|--------------------------------|------------------------------|-----------------------------|------|
| 30-30-30-30-30 | 5A-R1 | 4 | 45 | 48.1 | 84.0 | 1.75 | |
| | 5A-R2 | 4 | 90 | | 78.0 | 1.62 | |
| | 5A-R3 | 4* | | | 79.8 | 1.66 | |
| | 5C-R1 | 4 | 90 | 0.60/0.40 | 70.7 | 92.6 | 1.31 |
| | | 4* | | | 88.5 | 1.25 | |
| | | 2 | | | 80.2 | 1.13 | |
| | 5C-R2 | 2* | | | 80.3 | 1.14 | |
| 30-30-30-30-30-30-30-30 | 7A-R | 3 | 90 | 0.62/0.40 | 75.1 | 105 | 1.40 |
| 30-30-30-30-30-30-30-30 | 7C-R | 3 | | 0.57/0.40 | 72.9 | 100 | 1.37 |

* Reinforcement applied from top of the plate

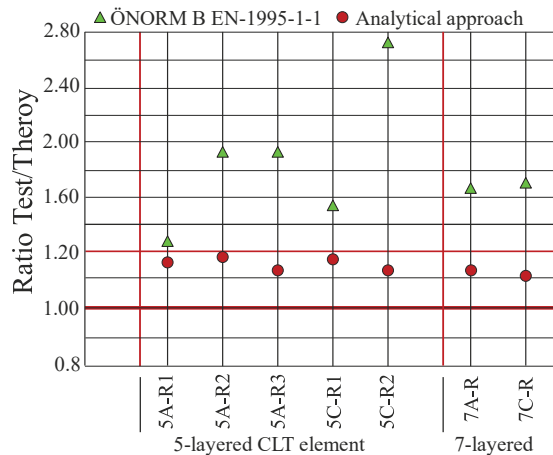


Figure 22: Comparison of the load-bearing capacity from the experimental tests and the analytical models

6 CONCLUSIONS

In this paper a contribution for prediction of the force in the reinforcement and the load-bearing capacity in reinforced notched CLT plates is given. In general, notches should be avoided due to the severe impact on the load-bearing capacity, robustness and ductility of load-bearing timber members, but if used they should be reinforced in any case.

The proposed way of reinforcing notched CLT plates is with self-tapping screws placed in one row at a maximum distance $a_1 = 150$ mm and distance $a_{3c} = 2.5 \cdot d_{screw}$ from the notch tip. A force in the screw can be calculated with Eq. (5), assuming a conservative crack length $L_{crack} = H$, for simplification. The current method for unlayered reinforced notches in the National Annexes [3] and [4] to EC-1995-1-1 also potentially show a possibility to predict the force in the reinforcement of notched CLT plates. However, more investigations should be conducted. Nonetheless, it is questionable, if such mechanical inconsistent approaches should be utilized in standards and guidelines for CLT after all.

An explicit and mechanically consistent analytical model for the prediction of the load-bearing capacity in reinforced notches of CLT plates was presented. The analytical model showed a good accuracy with the numerical model in scope of mode mixity, being important for the determination of the load-bearing capacity. The analytical model also showed a good correspondence with conducted experimental results. Nonetheless the analytical approach should be further refined and simplified as much as possible in order to be applicable in standards and guidelines.

For a further refinement of the analytical model, it would be of interest to apply fracture mechanics based methods of higher order, e.g. Zig-Zag theory, as the shear in the transversal layers has a big influence on the deformations at the crack tip and therefore on the load-bearing capacity. For the future work it is essential to conduct additional experimental tests on reinforced notched CLT plates including a wide range of different layouts and parameters ω and β in order to further verify the given proposals.

ACKNOWLEDGEMENT

This research work was prepared within the frame of the project "Notches in CLT and CLT ribbed panels" which was funded in the program line FFG Collective Research by the Austrian Research Promotion Agency FFG. The work of Erik Serrano was part of the project InnoCrossLam, supported under the umbrella of ERA-NET Cofund ForestValue.

REFERENCES

- [1] Jockwer, R.: Structural Behaviour of Glued Laminated Timber Beams with Unreinforced and Reinforced Notches, Dissertation, ETH Zurich, 2014
- [2] EN 1995-1-1:2004: Design of timber structures - Part 1-1: General and rules for buildings. CEN.
- [3] DIN EN 1995-1-1/NA:2013: Nationaler Anhang - National festgelegte Parameter - Eurocode 5: Bemessung und Konstruktion von Holzbauten - Teil 1-1: Allgemeines - Allgemeine Regeln und Regeln für den Hochbau
- [4] ÖNORM B 1995-1-1:2019: Bemessung und Konstruktion von Holzbauten, Teil 1-1: Allgemeines - Allgemeine Regeln und Regeln für den Hochbau, Ausgabe: 2019-06-01.
- [5] Henrici, D.: Beitrag zur Spannungsermittlung in ausgeklinkten Biegeträgern aus Holz, PhD thesis, Technische Universität München, Germany, 1984.
- [6] prEN 1995-1-1:20XX: Comment on consolidated draft prEN 1995-1-1, informal enquiry, CEN/TC 250/SC 5 "Eurocode 5: Design of timber structures"
- [7] Dietsch, P.: Reinforcement of Timber Structures-a New Section for Eurocode 5, in World conference on Timber Engineering, Vienna, Austria, 2016.
- [8] Jockwer, R., et.al.: Enhanced design approach for reinforced notched beams, 46th CIB-W18 Meeting, 26 to 29 August 2013, Vancouver, Canada, 2013.
- [9] Riipola, K.: Dimensioning of beams with cracks, notches and holes. An application of fracture mechanics, In: Proc. Of the CIB-W18 Meeting 23, Paper No. CIB-W18/a 23-19-1, Lisbon, Portugal, 1990
- [10] Sorin, E., Coureau J.L., Chaplain M.: Prediction of the ultimate load-carrying capacity of wooden notched beams with and without reinforcements using a splitting model. *Construction and Building Materials* 271 (2021) 121518, 2021
- [11] Ringhofer, A.; Screw Stiffness: highlights, Vortrag im Rahmen der Beiratssitzung des IHBV, 7.10.2021., Wien
- [12] Malagic A., Augustin M., Silly G., Thiel A., Schickhofer G.: Load-bearing Capacity and Fracture Behaviour of Notched Cross Laminated Timber Plates, in: International Network on Timber Engineering Research – Proceedings Meeting 54, Paper INTER/54-12-5, Online, 2021.
- [13] Blaß, H.J., Bejtka, I.: Querzugverstärkungen in gefährdeten Bereichen mit selbstbohrenden Holzschrauben. Deutsche Gesellschaft für Holzforschung, Universität Fridericiana Karlsruhe, Stuttgart, Germany, 2003
- [14] Serrano, E., Danielsson, H. (2020): Fracture Mechanics Based Design of CLT plates– Notches at Supports and Half and-Half Joints. In: International Network on Timber Engineering Research – Proceedings Meeting 53, Paper INTER/53-12-2, Online
- [15] Williams, J. G.: On the Calculation of Energy Release Rates for Cracked Laminates. *International Journal of Fracture* 36, 101-119, 1988.
- [16] Bennati, S., Fusicaro, P., Taglialigne, L., Valvo, P.S.: An Elastic Interface Model for the Delamination of Bending-Extension Coupled Laminates, Article in *Applied Sciences*, August, 2019